DOI: 10.1002/anie.201307619

Flexible Materials

A Highly Stretchable, Fiber-Shaped Supercapacitor**

*Zhibin Yang, Jue Deng, Xuli Chen, Jing Ren, and Huisheng Peng**

Flexible and portable devices are a mainstream direction in modern electronics and related multidisciplinary fields. To this end, they are generally required to be stretchable to satisfy various substrates.[1,2] As a result, stretchable devices, such as electrochemical supercapacitors,[3–6] lithium-ion batteries,[7] organic solar cells,[8] organic light-emitting diodes,[9,10] field-effect transistors,[11] and artificial skin sensors[12] have been widely studied. However, these stretchable devices are made in a conventional planar format that has largely hindered their development. For the portable applications, the devices need to be lightweight and small, though it is difficult for them to be made into efficient microdevices. In particular, it is challenging or even impossible for them to be used in electronic circuits and textiles that are urgently required also in a wide variety of other fields, such as microelectronic applications.

Recently, some attempts have been made to fabricate wire-shaped microdevices, such as electrochemical supercapacitors. They have been generally produced by twisting two fiber electrodes with electrolytes coated on the surface.[13–19] Several examples have been also successfully shown to make fiber-shaped supercapacitors with a coaxial structure.[20,21] Compared with their planar counterparts, the wire or fiber shape enables promising advantages such as being lightweight and woven into textiles. Although the wire and fiber-shaped supercapacitors are also flexible with high electrochemical performance, they are not stretchable, which is critically important for many applications. For instance, the resulting electronic textiles could easily break during the use if they were not stretchable.

To the best of our knowledge, herein we have, for the first time, developed a novel family of highly stretchable, fiber-shaped high-performance supercapacitors. Aligned carbon nanotube (CNT) sheets that are sequentially wrapped on an elastic fiber serve as two electrodes. The use of aligned CNT sheets offers combined remarkable properties including high flexibility, tensile strength, electrical conductivity, and mechanical and thermal stability. As a result, the fiber-shaped supercapacitor maintains a high specific capacitance of approximately 18 F/g after stretch by 75 % for 100 cycles.

Spinnable CNT arrays were first synthesized by chemical vapor deposition. A scanning electron microscopy (SEM) image of the array with height of 230 μm is shown in the Supporting Information, Figure S1, and the CNT shows a multi-walled structure with diameter of about 10 nm (Supporting Information, Figure S2). Aligned CNT sheets could be then continuously drawn from the array and easily attached to various substrates. Elastic fibers were used herein to offer the stretchability in the resulting supercapactiors, and rubber fibers have been mainly studied as a demonstration. For a typical fabrication on the fiber-shaped supercapacitor (Figure 1), a rubber fiber was first coated with a thin layer of

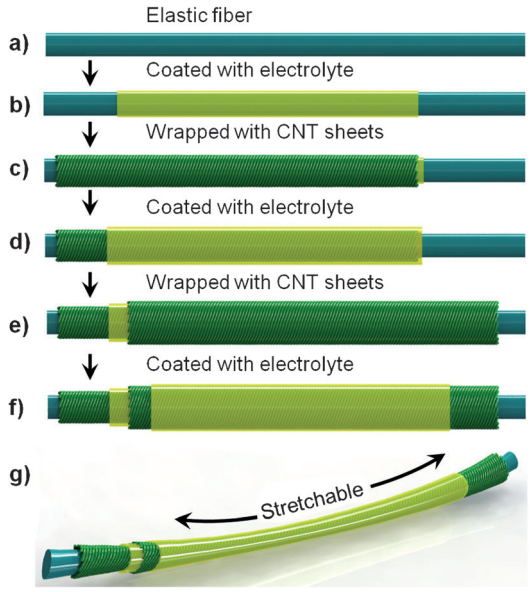

Figure 1. Illustration to the fabrication of a highly stretchable, fiber-shaped supercapacitor with a coaxial structure.

H_3PO_4–poly(vinyl alcohol) (PVA) gel electrolyte, followed by winding with a CNT sheet as the inner electrode, coating with the second layer of electrolyte, winding with another CNT sheet as the outer electrode that shares the same thickness with the inner electrode, and finally coating with the third layer of electrolyte. A vacuum treatment had been used to improve the infiltration of the electrolyte into the aligned CNTs after coat of the electrolyte. Figure 1 g shows the structure of the resulting supercapacitor. Similar to springs, the wrapped CNT sheet electrodes can well maintain the aligned structure as the CNTs are stabilized by the gel electrolyte during stretching. Both rubber fiber substrate and

[*] Z. Yang, J. Deng, X. Chen, J. Ren, Prof. H. Peng
State Key Laboratory of Molecular Engineering of Polymers
Department of Macromolecular Science and Laboratory of Advanced Materials
Fudan University, Shanghai 200438 (China)
E-mail: penghs@fudan.edu.cn

[**] This work was supported by the NSFC (91027025, 21225417), MOST (2011CB932503, 2011DFA51330), STCSM (11520701400, 12nm0503200), the Fok Ying Tong Education Foundation, The Program for Prof. of Special Appointment at Shanghai Institutions of Higher Learning, the Ministry of Education Ph.D. Scholar Award, and the Program for Outstanding Young Scholars from Organization Department of the CPC Central Committee.

Supporting information for this article is available on the WWW under http://dx.doi.org/10.1002/anie.201307619.

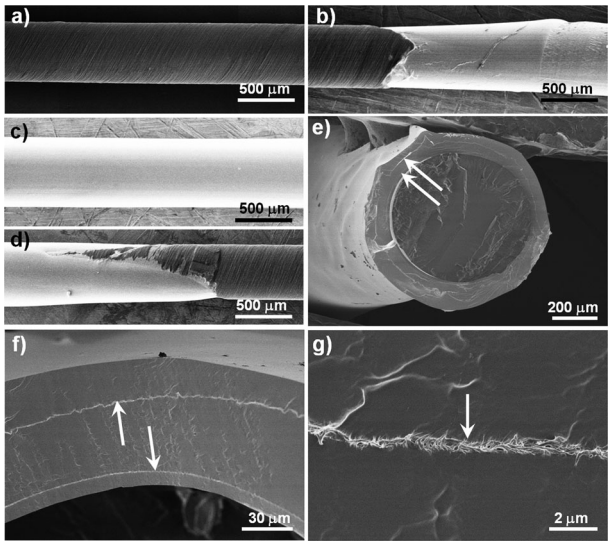

Figure 2. Scanning electron microscopy (SEM) images of fiber-shaped supercapacitors. a) The inner CNT sheet electrode that corresponds to the state at (c) in Figure 1. b)–d) SEM images of the left, middle, and right parts of the fiber-shaped supercapacitor corresponding to the state at (f) in Figure 1. e)–g) Cross-sectional images of a fiber-shaped supercapacitor with different magnifications. The arrows show the aligned CNT sheet.

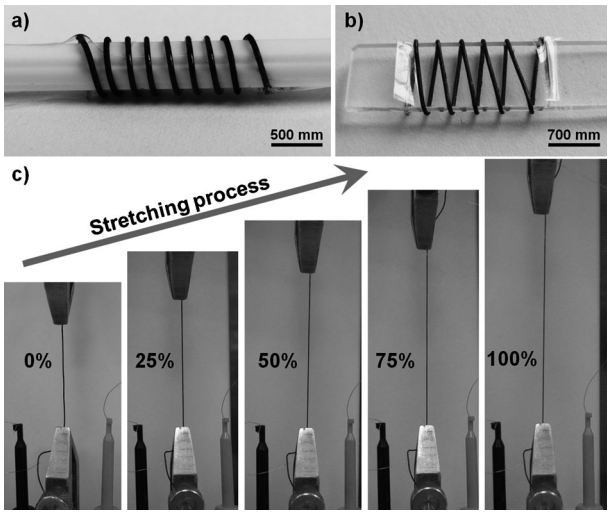

Figure 3. a), b) Photographs of two fiber-shaped supercapacitors being wound on different shapes of substrates. c) Photograph of the fiber-shaped supercapacitor with different strains of 0%, 25%, 50%, 75%, and 100%.

gel electrolyte are stretchable, so the supercapacitor also has the property of stretchability.

Figure 2a shows a typical SEM image of the first CNT layer that serves as the inner electrode in the fiber-shaped supercapacitor. Obviously the aligned CNT sheet has been uniformly and stably attached on the rubber fiber, which can be further confirmed by the high-resolution SEM image (Supporting Information, Figure S3). So does the second CNT layer that functions as the outer electrode. As a result, the fiber-shaped supercapacitor is uniform in diameter. Figure 2b,c,d shows typical SEM images of the left, middle, and right parts of a fiber-shaped supercapacitor with diameter of approximately 650 μm. The core–sheath structure has been further verified by the cross-sectional image of the supercapacitor (Figure 2e,f,g). The two CNT layers can be clearly observed to be separated by an electrolyte layer. The use of inner and outer electrolyte layers can improve the infiltration of the electrolyte among aligned CNTs. The innermost electrolyte layer also contributes to a strong attachment onto the rubber fiber (Supporting Information, Figure S4), while the outermost electrolyte layer can prevent the outer CNT sheet electrode from being damaged. These fiber-shaped supercapacitors were highly flexible, and no obvious damage in the structure had been traced by SEM observations after they were wound onto different substrates and shapes (Figure 3a,b). In particular, the use of the elastic rubber fiber and aligned CNT electrode provides the supercapacitor with highly stretchability (Supporting Information, Video S1). Figure 3c (see also the Supporting Information, Figure S5) shows that a fiber-shaped supercapacitor can be easily stretched by 100% without an obvious decrease in the structure integrity. To further verify the high stretchability and structural stability, the electrical resistance of the rubber fiber attached with aligned CNT sheets was traced during the stretching process. Interestingly, a micro-buckled structure was observed on the above fiber and the electrical resistance was varied in less than 5% during stretch with a strain of 100% (Supporting Information, Figures S6, S7). These properties are critically important to guarantee a high specific capacitance and stability during use.

Different thicknesses of CNT layers, that is, 110, 220, 330, 440, and 550 nm, were compared for the fiber-shaped supercapacitors. The thickness was controlled by varying the layer number of aligned CNT sheets, which typically have a thickness of about 18 nm.[22] Cyclic voltammetry (CV) was first used to characterize the electrochemical property of aligned CNT electrodes.[23] Figure 4a shows typical CV curves that were measured by a two-electrode system at a scan rate of 50 $mV\,s^{-1}$ in the PVA/H_3PO_4 gel electrolyte. Obviously, the CV curves share a rectangular shape that corresponds to an electrochemical double-layer capacitor. The current was first increased with the increasing thickness of CNT electrode from 110 to 330 nm and then maintained with the further increase in the thickness. The increasing current is mainly derived from the higher electrode mass, while the formation of a platform may be explained by the fact that it is difficult for the gel electrolyte to infiltrate into the dense CNT material. Figure 4b shows the corresponding galvanostatic charge–discharge curves of the supercapacitor between 0 and 0.8 V at a current density of 0.1 $A\,g^{-1}$. The charge-discharge curves were nearly symmetric, which indicated a high reversibility between charge and discharge processes. Figure 4c compares the specific capacitances of the aligned CNT electrodes with increasing thicknesses. They increased from 11.0 to 19.2 $F\,g^{-1}$ with the increasing thickness from 110 to 330 nm, which is mainly due to the decreased electrical resistance of the CNT sheet electrode. With the further increase to 550 nm, the capacitances are reduced to 11.3 $F\,g^{-1}$ as the gel electrolyte cannot be efficiently infiltrated into the CNT sheet electrode during the fabrication. Obviously, an optimal thickness for the

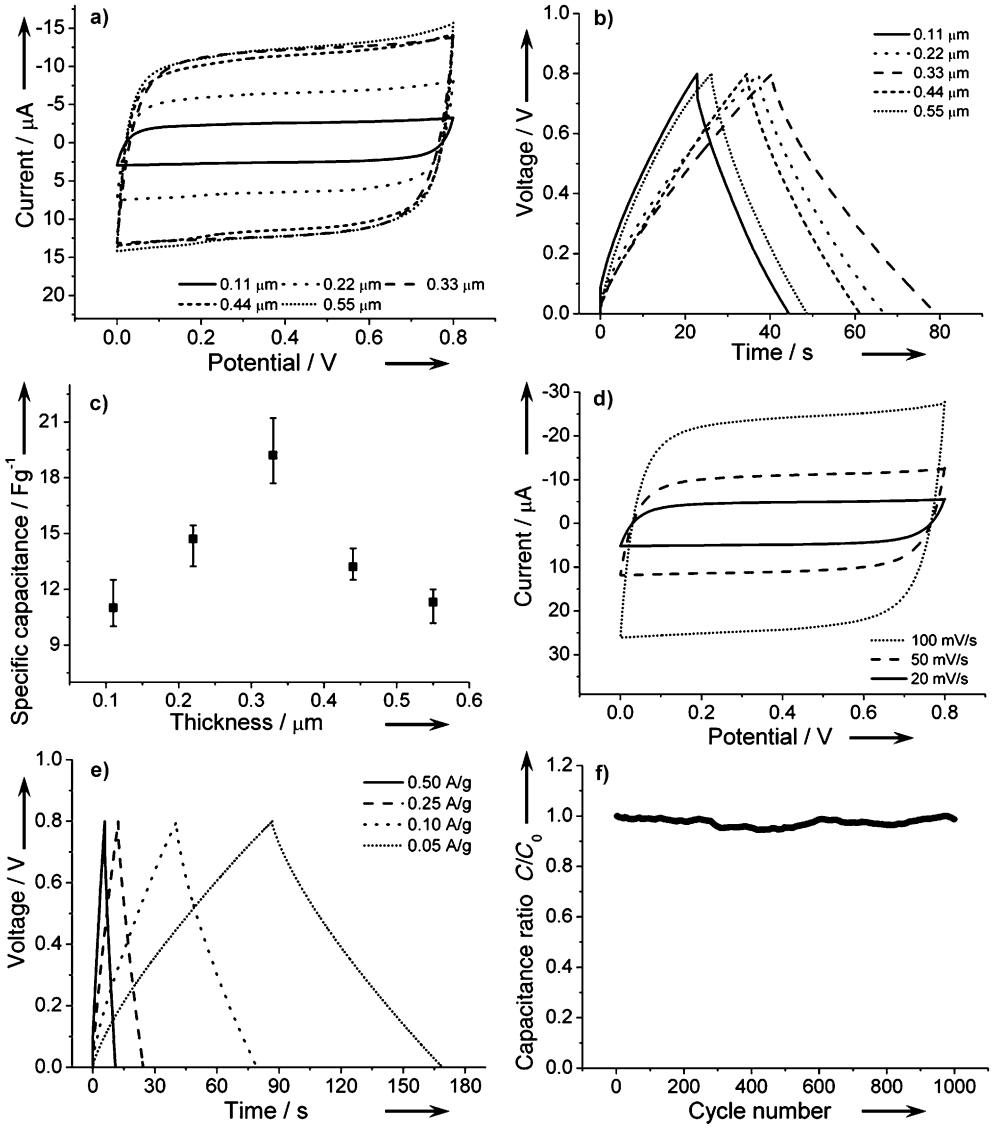

Figure 4. a), b) CV and Galvanostatic charge–discharge curves of fiber-shaped supercapacitors with different thicknesses of CNT layers. The CV measurements were performed in a potential range of 0 to 0.8 V at a scan rate of 50 $mV s^{-1}$ in H_3PO_4–PVA gel electrolyte. The Galvanostatic charge–discharge measurements were carried out at a current density of 0.1 $A g^{-1}$. c) Dependence of specific capacitance on the thickness of CNT layer. d) CV curves of a fiber-shaped supercapacitor with the CNT thickness of 0.33 μm at different scan rates. e) Galvanostatic charge–discharge curves of a fiber-shaped supercapacitor with the CNT thickness of 0.33 μm at different current densities. f) Dependence of specific capacitance on cycle number for a fiber-shaped supercapacitor with the CNT thickness of 0.33 μm. The specific capacitance was calculated from the charge–discharge curves at the current density of 0.1 $A g^{-1}$ in H_3PO_4–PVA gel electrolyte.

CNT electrode appears at 330 nm for the fiber-shaped supercapacitor.

Figure 4d compares CV curves of the fiber-shaped supercapactor based on the 330 nm-thick CNT electrodes with increasing scan rates from 20 to 100 $mV s^{-1}$. The rectangular shape is well-maintained, which indicates a high electrochemical stability in the supercapacitor. Figure 4e further shows the charge–discharge curves at different current densities from 0.05 to 0.50 $A g^{-1}$. The charge–discharge curves are similar in shape between 0 and 0.8 V, indicating that the supercapacitors can be stably performed in a wide range of current densities. The specific capacitances have been maintained to be almost 100% after 1000 charge–discharge cycles (Figure 4f). To better understand the stable electrochemical performance, the structure of the supercapacitor was further traced by SEM, and it was found to be well-maintained after operation (Supporting Information, Figure S8).

The dependence of specific capacitance on supercapacitor length had been also carefully investigated aiming at practical applications. The specific capacitances were slightly varied at about 20 $F g^{-1}$ with the increasing length from 2 to 10 cm (Supporting Information, Figure S9). The mass energy and power densities of the fiber-shaped supercapacitor are further compared in the Supporting Information, Figure S10. The mass energy densities are decreased from 0.515 to 0.363 $Wh kg^{-1}$, while the mass power densities are increased from 19 to 421 $W kg^{-1}$ with the increasing charge–discharge current density from 0.05 to 1 $A g^{-1}$.

The specific capacitance can be further enhanced by introducing ordered mesoporous carbon (OMC) components among aligned CNTs in the two electrodes by a dip-coating method (Supporting Information, Figure S11). CV curves of the supercapacitors fabricated with different OMC contents in the CNT composite electrodes are shown in the Supporting Information, Figure S12; the current increases with increasing OMC weight percentage. Corresponding charge–discharge curves of the supercapactiors measured at a current density of 0.1 $A g^{-1}$ are given in the Supporting Information, Figure S13a. The specific capacitance is improved to 41.4 $F g^{-1}$ at the aligned CNT/OMC composite layer with an OMC weight percentage of 50%, compared with 19.2 $F g^{-1}$ without the use of OMC (Supporting Information, Figure S13b).

Some attempts have been made to fabricate supercapacitors based on carbon-based fiber electrodes. In the case of

CNT materials, the specific capacitances were typically low, for example, 4.5 and 5 $F g^{-1}$.[24,25] The fiber-shaped supercapacitors based on graphene and pen ink were 25–40[14] and 21–35 $F g^{-1}$,[13] respectively. For a carbon nanofiber/CNT composite, the resulting fiber-shaped supercapacitors exhibited specific capacitances of 42–80 $F g^{-1}$.[20] In summary, herein the stretchable fiber-shaped supercapacitors show the similar level of specific capacitances to the other carbon-based fiber-shaped supercapacitors that were not stretchable.

The electrochemical properties of the fiber-shaped supercapacitor were carefully studied for the high flexibility and stretchability. Here the bare aligned CNT electrode has been studied as a demonstration. The CV and charge–discharge curves of the fiber-shaped supercapacitors being bent with different radii of curvatures are compared in Figure 5a (see also the Supporting Information, Figure S14). The shapes of CV and charge–discharge curves were maintained to be almost the same under all bending conditions. The CV and charge–discharge curves of the fiber-shaped supercapacitors by stretch with different strains are further compared in Figure 5b (see also the Supporting Information, Figure S15). The CV and charge-discharge curves remain unchanged at a strain of 75% or lower and start to deform at a higher value. Furthermore, the specific capacitance is maintained by more than 95% after stretched by 100 cycles at a strain of 75% without obvious structural damages (Figure 5c; Supporting Information, Figure S16). Furthermore, it can be also remained above 90% after 1000 charge-discharge cycles when applied a strain of 75% (Figure 5d).

In summary, a highly stretchable, fiber-shaped supercapacitor has been developed with high performance by winding aligned CNT sheets on elastic fibers. The high stretchability and specific capacitance have been simultaneously achieved by designing a coaxial structure that favors high contact areas between the electrode and electrolyte besides the combined remarkable properties enabled by the aligned CNTs.

Received: August 29, 2013
Published online: November 8, 2013

Keywords: conductive materials · elastic fibers · stretchable materials · supercapacitors

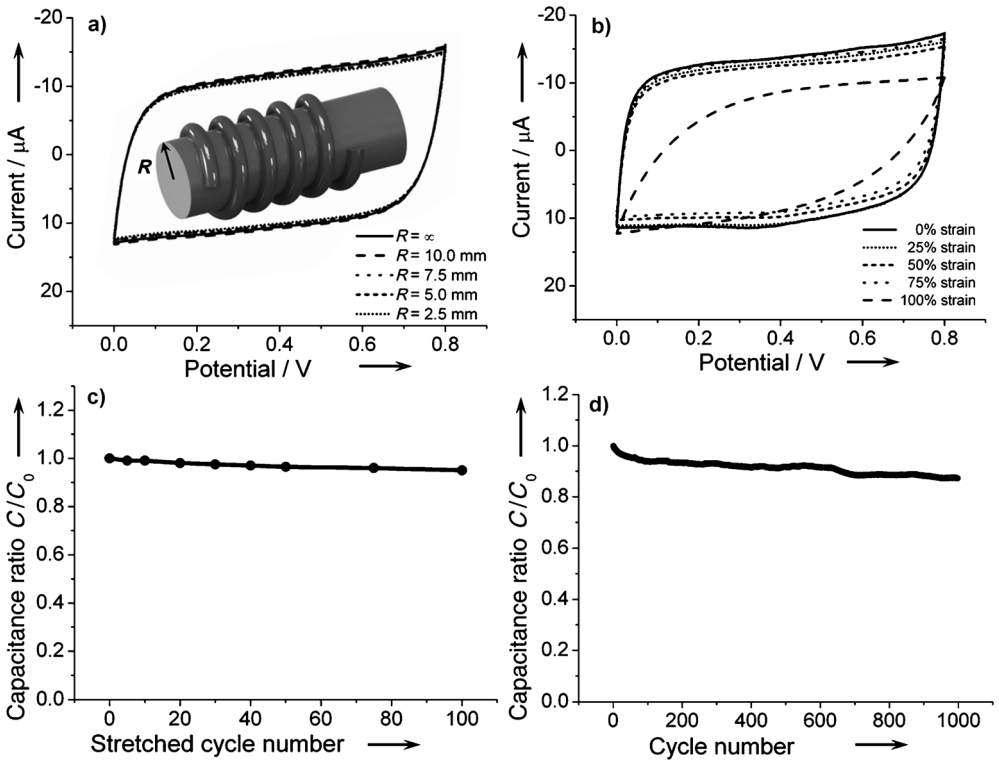

Figure 5. a) CV curves of the fiber-shaped supercapacitor without bending (labeled with ∞) and being bent with different radii *R* of curvatures. b) CV curves of the fiber-shaped supercapacitor with increasing strains from 0 to 100%. c) Dependence of specific capacitance on stretched cycle number with a strain of 75%. d) Dependence of specific capacitance on cycle number with a strain of 75%. C_0 and *C* in (c) and (d) correspond to specific capacitances before and after different cycles, respectively. The supercapacitor was fabricated from the CNT layer with a thickness of 0.33 μm. The CV measurements were performed at a potential range of 0 to 0.8 V with a scan rate of 50 $mV s^{-1}$ in H_3PO_4–PVA gel electrolyte.

[1] J. A. Rogers, T. Someya, Y. Huang, *Science* **2010**, *327*, 1603–1607.
[2] D. J. Lipomi, Z. Bao, *Energy Environ. Sci.* **2011**, *4*, 3314–3328.
[3] Z. Niu, H. Dong, B. Zhu, J. Li, H. H. Hng, W. Zhou, X. Chen, S. Xie, *Adv. Mater.* **2013**, *25*, 1058–1064.
[4] C. Yu, C. Masarapu, J. Rong, B. Wei, H. Jiang, *Adv. Mater.* **2009**, *21*, 4793–4797.
[5] L. Hu, M. Pasta, F. L. Mantia, L. Cui, S. Jeong, H. D. Deshazer, J. W. Choi, S. M. Han, Y. Cui, *Nano Lett.* **2010**, *10*, 708–714.
[6] X. Li, T. Gu, B. Wei, *Nano Lett.* **2012**, *12*, 6366–6371.
[7] S. Xu, Y. Zhang, J. Cho, J. Lee, X. Huang, L. Jia, J. A. Fan, Y. Su, J. Su, H. Zhang, *Nat. Commun.* **2013**, *4*, 1543.
[8] D. J. Lipomi, B. C. K. Tee, M. Vosgueritchian, Z. Bao, *Adv. Mater.* **2011**, *23*, 1771–1775.
[9] Z. Yu, X. Niu, Z. Liu, Q. Pei, *Adv. Mater.* **2011**, *23*, 3989–3994.
[10] T. Sekitani, H. Nakajima, H. Maeda, T. Fukushima, T. Aida, K. Hata, T. Someya, *Nat. Mater.* **2009**, *8*, 494–499.
[11] S. H. Chae, W. J. Yu, J. J. Bae, D. L. Duong, D. Perello, H. Y. Jeong, Q. H. Ta, T. H. Ly, Q. A. Vu, M. Yun, *Nat. Mater.* **2013**, *12*, 403–409.
[12] D. J. Lipomi, M. Vosgueritchian, B. C. Tee, S. L. Hellstrom, J. A. Lee, C. H. Fox, Z. Bao, *Nat. Nanotechnol.* **2011**, *6*, 788–792.

[13] Y. Fu, X. Cai, H. Wu, Z. Lv, S. Hou, M. Peng, X. Yu, D. Zou, *Adv. Mater.* **2012**, *24*, 5713 – 5718.
[14] Y. Meng, Y. Zhao, C. Hu, H. Cheng, Y. Hu, Z. Zhang, G. Shi, L. Qu, *Adv. Mater.* **2013**, *25*, 2326 – 2331.
[15] J. Ren, L. Li, C. Chen, X. Chen, Z. Cai, L. Qiu, Y. Wang, X. Zhu, H. Peng, *Adv. Mater.* **2013**, *25*, 1155 – 1159.
[16] K. Wang, Q. Meng, Y. Zhang, Z. Wei, M. Miao, *Adv. Mater.* **2013**, *25*, 1494 – 1498.
[17] J. Bae, M. K. Song, Y. J. Park, J. M. Kim, M. Liu, Z. L. Wang, *Angew. Chem.* **2011**, *123*, 1721 – 1725; *Angew. Chem. Int. Ed.* **2011**, *50*, 1683 – 1687.
[18] T. Chen, L. Qiu, Z. Yang, Z. Cai, J. Ren, H. Li, H. Lin, X. Sun, H. Peng, *Angew. Chem.* **2012**, *124*, 12143 – 12146; *Angew. Chem. Int. Ed.* **2012**, *51*, 11977 – 11980.
[19] J. A. Lee, M. K. Shin, S. H. Kim, H. U. Cho, G. M. Spinks, G. G. Wallace, M. D. Lima, X. Lepró, M. E. Kozlov, R. H. Baughman, *Nat. Commun.* **2013**, *4*, 1970.
[20] V. T. Le, H. Kim, A. Ghosh, J. Kim, J. Chang, Q. A. Vu, D. T. Pham, J.-H. Lee, S.-W. Kim, Y. H. Lee, *ACS Nano* **2013**, *7*, 5940 – 5947.
[21] G. Sun, L. Zheng, J. An, Y. Pan, J. Zhou, Z. Zhan, J. H. Pang, C. K. Chua, K. Leong, L. Li, *Nanoscale* **2013**, *5*, 2870 – 2874.
[22] Z. Yang, T. Chen, R. He, G. Guan, H. Li, L. Qiu, H. Peng, *Adv. Mater.* **2011**, *23*, 5436 – 5439.
[23] Y. Tan, C. Xu, G. Chen, Z. Liu, M. Ma, Q. Xie, N. Zheng, S. Yao, *ACS Appl. Mater. Interfaces* **2013**, *5*, 2241 – 2248.
[24] A. B. Dalton, S. Collins, E. Munoz, J. M. Razal, V. H. Ebron, J. P. Ferraris, J. N. Coleman, B. G. Kim, R. H. Baughman, *Nature* **2003**, *423*, 703 – 703.
[25] Z. Cai, L. Li, J. Ren, L. Qiu, H. Lin, H. Peng, *J. Mater. Chem. A* **2013**, *1*, 258 – 261.

